# Numerical study of two disks settling in an Oldroyd-B fluid: From periodic interaction to chaining

Tsorng-Whay Pan and Roland Glowinski

# Numerical study of two disks settling in an Oldroyd-B fluid: From periodic interaction to chaining

Tsorng-Whay Pan

*Department of Mathematics, University of Houston, Houston, Texas 77204, USA*

Roland Glowinski

*Department of Mathematics, University of Houston, Houston, Texas 77204, USA*
*Department of Mathematics, Hong Kong Baptist University, Hong Kong*

## Abstract

In this article we present a numerical study of the dynamics of two disks sedimenting in a narrow vertical channel filled with an Oldroyd-B fluid. Two kinds of particle dynamics are observed: (i) a periodic interaction between the two disks, and (ii) the formation of a two disk chain. For the periodic interaction of the two disks, two different motions are observed: (a) the two disks stay far apart and interact periodically, and (b) the two disks interact closely and then far apart in a periodic way, like the drafting, kissing and tumbling of two disks sedimenting in a Newtonian fluid, due to a weak elastic force. Concerning the formation of two disk chain occurring at higher values of the elasticity number, either a tilted chain or a vertical chain are observed. Our simulations show that, as expected, the values of the elasticity and Mach numbers are the determining factors concerning the particle chain formation and its orientation.

**Keywords:** Sedimentation, Particle chaining, Periodic motion, Oldroyd-B viscoelastic fluids

## 1    Introduction

The motion of particles in non-Newtonian fluids is not only of fundamental theoretical interest, but is also of importance in many applications to industrial processes involving particle-laden materials (see, e.g., [1] and [2]). For example, during the hydraulic fracturing operation used in oil and gas wells, suspensions of solid particles in polymeric solutions are pumped into hydraulically-induced fractures. The particles must prop these channels open to enhance the rate of oil recovery [3]. During the shut-in stage, proppant settling is pronounced when the fluid pressure decreases due to the end of hydraulic fracturing process. The study of particle chain during settling in vertical channel can help us to understand the mechanism of proppant agglomeration in narrow fracture zones. There have been works on the simulation of the sedimentation of particles in Oldroyd-B fluids in, e.g., [4], [5], [6], [7], [8], [9], [10], further references being given in the review article [11]. Feng et al. [4] studied numerically the two-dimensional sedimentation of circular particles in an Oldroyd-B fluid:

---

these authors obtained chains of two particles aligned with the direction of sedimentation, which are precisely the kind of micro-structures observed in actual experiments [12]. In [6], an arbitrary Lagrangian-Eulerian (ALE) moving mesh technique (see [5]) was used to investigate the cross-stream migration and orientations of elliptic particles in Oldroyd-B fluids (with and without shear thinning). Huang *et al.* found that the orientation of elliptic particles depends on two critical numbers, the elasticity and Mach numbers. In [7], a fictitious domain/distributed Lagrange multiplier (FD/DLM) method for the numerical simulation of particulate flow of Oldroyd-B fluids was developed: chains of two particles aligned with the direction of sedimentation were obtained, and in the case of multiple circular particles, many two particle chains were observed next to the channel walls. Yu *et al.* [8] applied also a FD/DLM based methodology to study disk interactions in Oldroyd-B fluids, preliminary results concerning the attraction of two disks being reported. They obtained that two disks attract each other and form either a horizontal chain or tilted chain quickly while settling in an Oldroyd-B fluid instead of repelling each other as in a Newtonian fluid. Later on, Shao and Yu [9] used an improved FD/DLM method to show that the stable configuration is the one where the particles are aligned parallel to the flow direction when the Mach and elasticity numbers are in the range identified in [6].

In this article, we have further investigated the formation and orientation of two disk chains versus the values of the elasticity and Mach numbers via direct numerical simulation. Our results agree with those about the settling of an elliptic particle in Oldroyd-B fluids obtained in [6]. This kind of particle behavior is not surprising since these two particle chains behave as elongated bodies, despite the fact that the particles are loosely coupled. However, we observed also that if the elasticity number is sufficiently small, there are two new dynamical regimes, namely (i) the two disks stay far apart and their interaction is periodical and (ii) the two disks draft, kiss and break away periodically. Concerning the wall effect on the particle chains, we found that the formation of vertical chains can be obtained in a narrower channel for lower elasticity numbers. Also it is easier for two disks of slightly different sizes to form a chain when comparing to the case of two disks of same sizes. But when comparing with the dynamics of two rigidly connected disks sedimenting in an Oldroyd-B fluid, we have obtained that, as expected, the critical elasticity number for having vertical chain of two disks is much higher than that for two rigidly connected disks since the chain of two disks is not really a long rigid body. The article is organized as follows. In Section 2, we present a FD/DLM formulation for Oldroyd-B particulate flows and briefly discuss its space-time discretization by a methodology combining operator-splitting and finite element methods. In Section 3, we present and comment the results of the numerical experiments simulating the sedimentation of two disks.

## 2 Mathematical formulations and numerical methods

Although numerical methods for simulating particulate flows in Newtonian fluids have been very successful (e.g., see [13], [14], and [15]), numerically simulating particulate flows in viscoelastic fluids is a much more complicated and challenging issue. One of the difficulties (e.g., see [16], [17]) concerning the simulation of viscoelastic flows is the breakdown of the numerical methods. It is widely believed that the lack of positive definiteness preserving property of the conformation tensor at the discrete level during the *entire time integration*

is one of the reasons of this breakdown. To preserve the positive definiteness property of the conformation tensor, several methods have been proposed recently, as in [18], [19], [20] and [21]. In particular, Lozinski and Owens [21] factored the conformation tensor to get $\boldsymbol{\sigma} = \mathbf{A}\mathbf{A}^t$ and then wrote down the equations for $\mathbf{A}$ approximately at the discrete level, forcing the positive definiteness of the conformation tensor. The methods developed in [21] have been applied in [10] together with the FD/DLM method through operator splitting for simulating particulate flows in Oldroyd-B fluids. In this article, we present the results of numerical experiments concerning the simulation of two disks settling in an Oldroyd-B fluid; these results have been obtained using the numerical methods developed in [10].

## 2.1 Governing equations and their FD/DLM formulation

Following reference [10], we will address first the models and computational methodologies to be used in this article. Let $\Omega$ be a bounded two-dimensional (2D) region and let $\Gamma$ be its boundary. We suppose that $\Omega$ is filled with a viscoelastic Oldroyd-B fluid of density $\rho_f$ and contains $N$ moving rigid particles of density $\rho_s$ (see Figure 1). Let $B(t) = \cup_{i=1}^{N} B_i(t)$ where $B_i(t)$ is the $i$th rigid particle in the fluid for $i = 1, \ldots, N$. We denote by $\partial B_i(t)$ the boundary of $B_i(t)$. For some $T > 0$, the governing equations for the fluid-particle system are

$$\rho_f(\frac{\partial \mathbf{u}}{\partial t} + (\mathbf{u} \cdot \boldsymbol{\nabla})\mathbf{u}) = \rho_f \mathbf{g} - \boldsymbol{\nabla} p + 2\mu \boldsymbol{\nabla} \cdot \mathbf{D}(\mathbf{u}) + \boldsymbol{\nabla} \cdot \boldsymbol{\sigma}^p \ \ in \ \Omega \backslash \overline{B(t)}, \, t \in (0, T), \quad (1)$$

$$\nabla \cdot \mathbf{u} = 0 \ \ in \ \Omega \backslash \overline{B(t)}, \, t \in (0, T), \quad (2)$$

$$\mathbf{u}(\mathbf{x}, 0) = \mathbf{u}_0(\mathbf{x}), \quad \forall \mathbf{x} \in \Omega \backslash \overline{B(0)}, \ with \ \nabla \cdot \mathbf{u}_0 = 0, \quad (3)$$

$$\mathbf{u} = \mathbf{g}_0 \ \ on \ \Gamma \times (0, T), with \int_{\Gamma} \mathbf{g}_0 \cdot \mathbf{n} \, d\Gamma = 0, \quad (4)$$

$$\mathbf{u} = \mathbf{V}_{p,i} + \omega_i \ \overrightarrow{\mathbf{G}_i \mathbf{x}}^{\perp}, \ \forall \mathbf{x} \in \partial B_i(t), \, i = 1, \cdots, N, \quad (5)$$

$$\frac{\partial \mathbf{C}}{\partial t} + (\mathbf{u} \cdot \boldsymbol{\nabla}) \, \mathbf{C} - (\boldsymbol{\nabla}\mathbf{u}) \, \mathbf{C} - \mathbf{C} \, (\boldsymbol{\nabla}\mathbf{u})^t = -\frac{1}{\lambda_1}(\mathbf{C} - \mathbf{I}) \ \ in \ \Omega \backslash \overline{B(t)}, \, t \in (0, T), \quad (6)$$

$$\mathbf{C}(\mathbf{x}, 0) = \mathbf{C}_0(\mathbf{x}), \, \mathbf{x} \in \Omega \backslash \overline{B(0)}, \quad (7)$$

$$\mathbf{C} = \mathbf{C}_L(t), \ \ on \ \Gamma^-(t), \quad (8)$$

where $\mathbf{u}$ is the flow velocity, $p$ is the pressure, $\mathbf{g}$ denotes gravity, $\mathbf{D}(\mathbf{u}) = (\boldsymbol{\nabla}\mathbf{u} + (\boldsymbol{\nabla}\mathbf{u})^t)/2$ is the rate of deformation tensor, $\mu = \eta_1 \lambda_2 / \lambda_1$ is the solvent viscosity of the fluid, $\eta = \eta_1 - \mu$ is the elastic viscosity of the fluid, $\eta_1$ is the fluid viscosity, $\lambda_1$ is the relaxation time of the fluid, $\lambda_2$ is the retardation time of the fluid, $\mathbf{n}$ is the outer normal unit vector at $\Gamma$, $\Gamma^-(t)$ is the upstream part of $\Gamma$ at time $t$. The polymeric stress tensor $\boldsymbol{\sigma}^p$ in (1) is given by $\boldsymbol{\sigma}^p = \frac{\eta}{\lambda_1}(\mathbf{C} - \mathbf{I})$, where the conformation tensor $\mathbf{C}$ is symmetric and positive definite (see [24]) and $\mathbf{I}$ is the identity tensor.

In (5), the no-slip condition holds on the boundary of the $i$th particle, $\mathbf{V}_{p,i}$ is the translation velocity, $\omega_i$ is the angular velocity, $\mathbf{G}_i = \{G_{i,1}, G_{i,2}\}^t$ is the center of mass, and finally $\overrightarrow{\mathbf{G}_i \mathbf{x}}^{\perp} = \{-(y - G_{i,2}), (x - G_{i,1})\}^t$ for the rotation with respect to the mass center
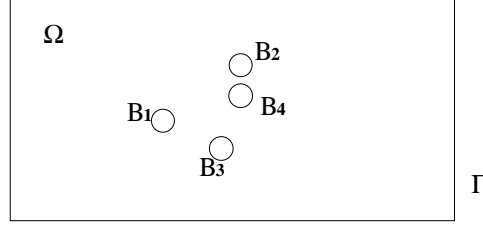
Figure 1: An example of a two-dimensional flow region with four circular particles.

$\mathbf{G}_i$ (for the 2D cases considered in this article). The motion of the particles is modeled by Newton's laws:

$$M_{p,i} \frac{d\mathbf{V}_{p,i}}{dt} = M_{p,i}\mathbf{g} + \mathbf{F}_i + \mathbf{F}_i^r, \tag{9}$$

$$I_{p,i}\frac{d\omega_i}{dt} = F_i^t, \tag{10}$$

$$\frac{d\mathbf{G}_i}{dt} = \mathbf{V}_{p,i}, \tag{11}$$

$$\mathbf{G}_i(0) = \mathbf{G}_i^0, \mathbf{V}_{p,i}(0) = \mathbf{V}_{p,i}^0, \omega_i(0) = \omega_i^0, \tag{12}$$

for $i = 1, \ldots, N$, where in (9)-(12), $M_{p,i}$ and $I_{p,i}$ are the the mass and the inertia of the $i$th particle, respectively, $\mathbf{F}_i^r$ is a short range repulsion force imposed on the $i$th particle by other particles and the wall to prevent particle/particle and particle/wall penetration (see [13] for details), and $\mathbf{F}_i$ and $F_i^t$ denote the hydrodynamic force and the associated torque imposed on the $i$th particle by the fluid, respectively.

In order to avoid frequent re-meshing and the difficulties associated with mesh generation on a time varying domain when the particles are very close to each others (a very common situation in 3D), we have used a fictitious domain approach extending the governing equations to the entire domain taken in [7, 13]. The basic idea of the fictitious domain method is to imagine that the fluid fills the entire space inside as well as outside the particle boundary. The fluid–flow problem is then posed on a larger domain (the"fictitious domain"). The fluid inside the particle boundary must exhibit a rigid–body motion. This constraint is enforced using the distributed Lagrange multiplier, which represents the additional body force per unit volume needed to maintain the rigid–body motion inside the particle boundary, much like the pressure in incompressible fluid flow, whose gradient is the force required to maintain the constraint of incompressibility.

The method of numerical solution is actually a combination of a distributed Lagrange multiplier based fictitious domain method and an operator splitting method. For space discretization, we use $P_1$-iso-$P_2$, $P_1$ and $P_1$ finite elements for the velocity field, conformation tensor and pressure, respectively. The details of numerical methods for simulating the motion of disks sedimenting in Oldroyd-B fluids in a vertical two-dimensional channel are given in [10]. Applying the Lie scheme to the discrete analogue of the DLM/FD formulation obtained from (1)-(12), we have used a seven stage operator-splitting scheme reported in [10] to obtain the numerical results reported here, namely: In Stage 1, we use a Neumann preconditioned Uzawa/conjugate gradient algorithm to force (in a $L^2$ sense) the incom-
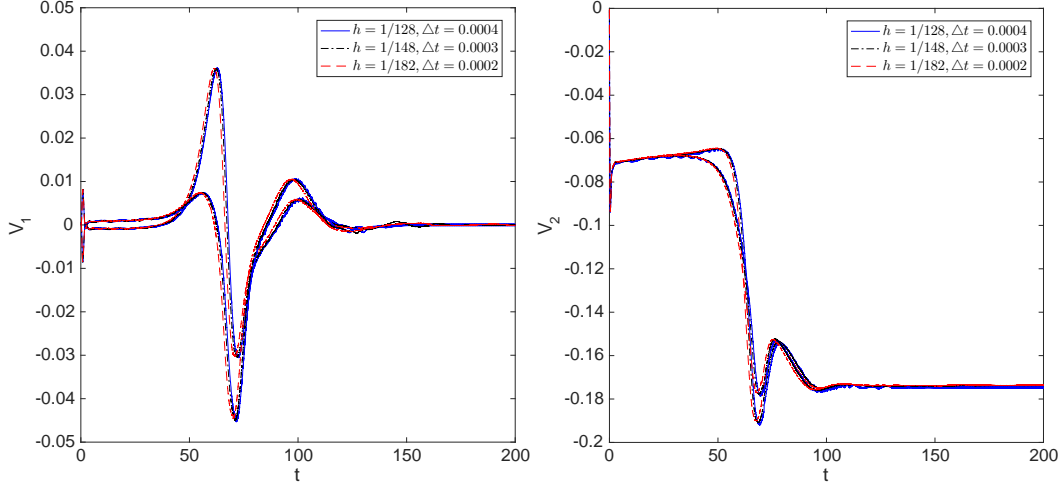
4

Figure 2: Histories of the two disk horizontal velocity (left) and vertical velocity (right) obtained by different mesh sizes and time steps for $\rho_s = 1.0025$ and E=0.8.

pressibility condition, $\boldsymbol{\nabla} \cdot \mathbf{u} = 0$, as discussed in [10] and [14]. In Stage 2, we combine two advection steps: one for $\mathbf{u}$ and one for $\mathbf{C}$, both are solved by a wave-like equation method (see [14] and [25]) which is explicit and does not introduce numerical dissipation. In this second stage, we have transformed the advection step for $\mathbf{C}$ into one for its Cholesky factor $\mathbf{A}$ (as advocated by Lozinski and Owens in [21]), taking advantage thus of the relation $\mathbf{C} = \mathbf{A}\mathbf{A}^t$. In Stage 3, we solve a diffusion step for $\mathbf{u}$ and then a step taking into account the remaining operator in the transformed evolution equation verified by $\mathbf{A}$. In Stage 4, we update the position of the disk mass center $\mathbf{G}$. In Stage 5, we force the rigid body motion of the particle and update $\mathbf{V}$ and $\omega$ by a conjugate gradient method described in, e.g., [10] and [14], and then impose the condition $\mathbf{C} = \mathbf{I}$ inside the particle. In Stage 6, we correct the position of $\mathbf{G}$ via the updated $\mathbf{V}$ and $\omega$. Finally, Stage 7 is a diffusion step for the velocity, driven by the updated polymeric stress tensor.

# 3   Numerical Results and discussion

In the following discussion, the particle Reynolds number is Re= $\dfrac{\rho_f U d}{\eta_1}$ and the Deborah number is De= $\dfrac{\lambda_1 U}{d}$ where $U$ is the averaged terminal velocity speed of disks and $d$ the disk diameter. The important combinations of Re and De are, as in [6],

$$\text{Mach number: M} = \sqrt{\text{DeRe}} = U/(\eta_1/\lambda_1 \rho_f)^{1/2},$$
$$\text{elasticity number: E} = De/Re = \lambda_1 \eta_1/d^2 \rho_f.$$

The Mach number is the ratio of the terminal velocity to the shear wave speed $c = (\eta_1/\lambda_1 \rho_f)^{1/2}$. The elasticity number depends on material parameters and particle size but is flow independent. It is the ratio of the elastic and inertia forces in the fluid. As discussed
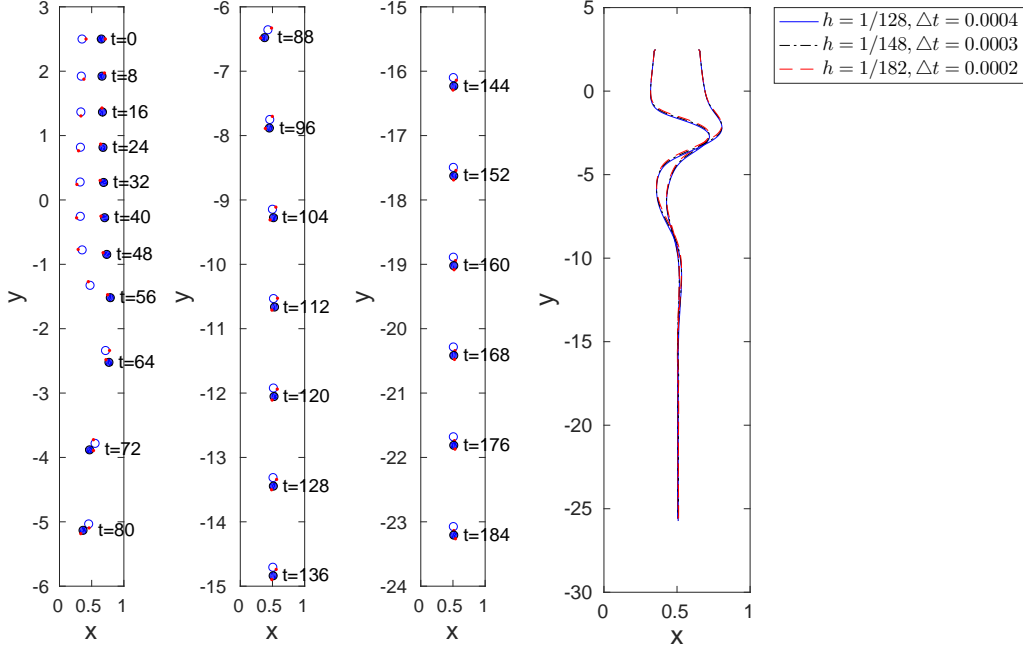
5

Figure 3: Positions of the two disks (left three) and trajectories of their centers (right) for $\rho_s = 1.0025$ and E=0.8.

in [6] and [26], when the elasticity number E is larger than a critical value ($O(1)$), a long body settling in Oldroyd-B fluids turns its broadside parallel to the flow direction. But for elasticity numbers E less than the critical value, this long body falls steadily in a configuration in which the axis of the long body is at a fixed angle of tilt with the horizontal direction. Also for larger Mach numbers, the long body flips into broadside on falling again. Concerning the dynamics of two disks settling in Oldroyd-B fluid, these two disks can be viewed as a long body if they form a chain. We intend to study the equilibrium orientation of this two disk chain, acting as a long body, by varying the elasticity number. However, since for E small enough the two disks may stay separated (no chain formation) ultimately, it is interesting to investigate how the two disks interact and how close is their interaction to the one of two disks settling in Newtonian fluid (exhibiting thus the drafting, kissing and tumbling phenomenon [22]), other possible outcomes being time periodic or chaotic interactions, as shown in [23]. We have used the numerical method developed in [10] to obtain the numerical results reported in this section.

In this article, we have considered the settling of two disks in a vertical channel of infinite length filled with an Oldroyd-B fluid as in [10]. We assume in this section that all dimensional quantities are in the CGS units. The computational domain is $\Omega = (0,1) \times (0,6)$ initially and then moves vertically with the mass center of the lowest disk (see, e.g., [27] and [28] and references therein for adjusting the computational domain according to the particle position). The two disk diameters are $d =0.125$ and the initial position of the disk centers are at (0.35, 2.5) and (0.65, 2.5), respectively. The disk density $\rho_s$ is 1.0025 for the first two cases considered in this section, the fluid density $\rho_f$ being 1. The fluid viscosity
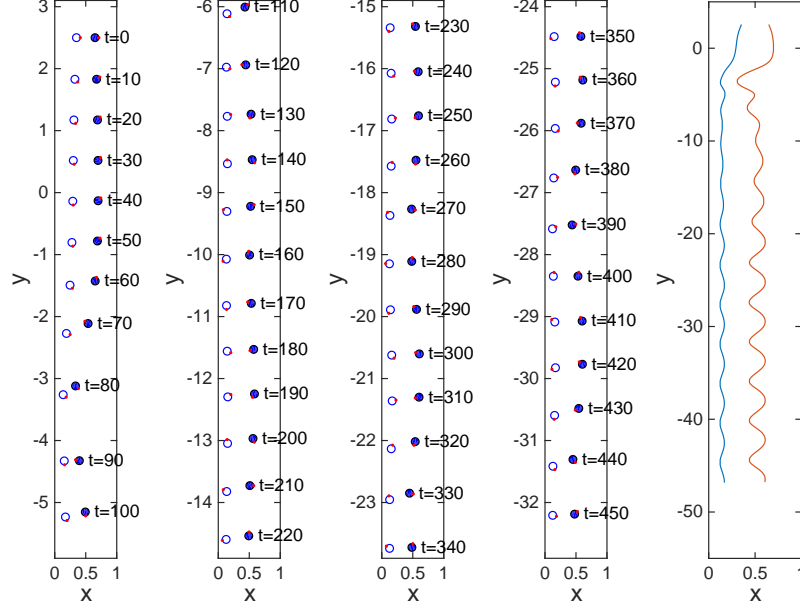
6

Figure 4: Positions of the two disks interacting apart (left four) and trajectories of their centers (right) for $\rho_s = 1.0025$ and E=0.16.
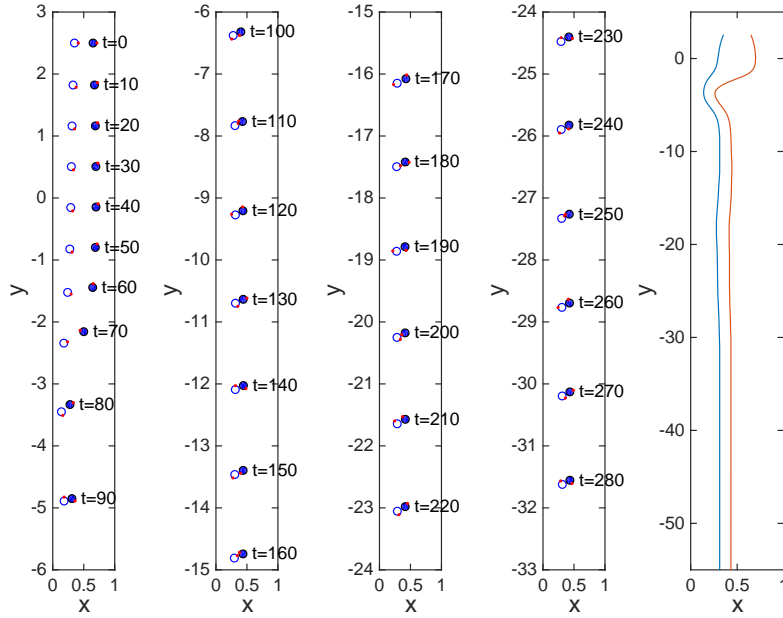


Figure 5: Positions of the two disks forming a tilted chain (left four) and trajectories of their centers (right) for $\rho_s = 1.0025$ and E=0.256.
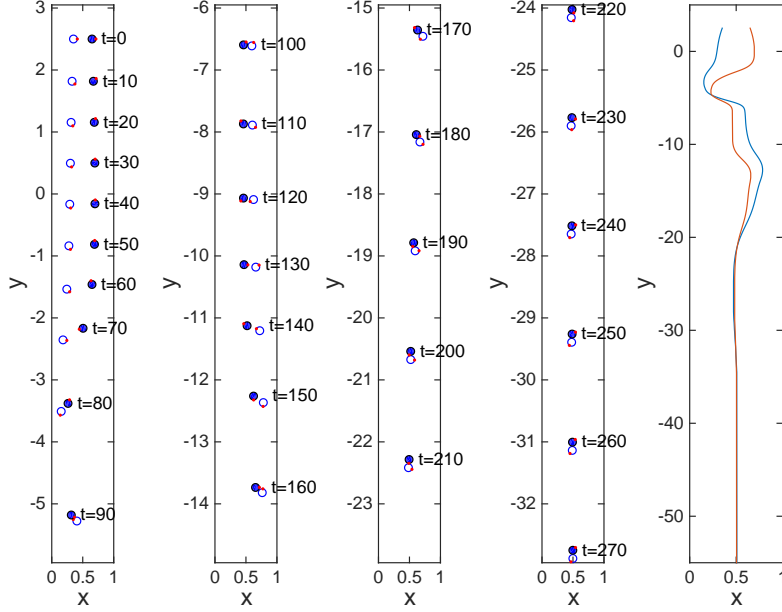
Figure 6: Positions of the two disks forming a vertical chain (left four) and trajectories of their centers (right) for $\rho_s = 1.0025$ and E=0.32.

$\eta_1$ is 0.025. The relaxation time $\lambda_1$ varies between 0.01 and 1.0 and the retardation time $\lambda_2$ is $\lambda_1/4$. Then the associated elasticity number is E=1.6$\lambda_1$. To validate the numerical methods, the case of two disks sedimenting in a vertical channel for the relaxation time $\lambda_1 = 0.5$ has been tested. In Figs. 2 and 3, the velocity and center trajectories of the two disks show that the convergence take place when reducing the mesh size and time step. The positions of the two disks shown in Fig. 3 present a typical interaction, drafting, kissing and chaining, for two disks settling in viscoelastic fluid.

For the following numerical results, the mesh sizes for the velocity field, conformation tensor and pressure are $h = 1/128$, $1/128$, and $1/64$, respectively, the time step being 0.0004. In Figs. 4, 5 and 6, three typical motions of two disks settling in an Oldroyd-B fluid are presented. For E=0.16 ($\lambda_1 = 0.1$), the two disk interaction dynamics is characterized by its periodical motion (of period 55.25 time units) as in Fig. 4, which is similar to the one, obtained in [23], for the motions of two disks settling in a Newtonian fluid. For a slightly higher value, E=0.256 ($\lambda_1 = 0.16$), the two disks form a chain with a stable tilt angle of 29.39 degrees (see Fig. 5), which is similar to the behavior of a long body when the elasticity number is less than the critical value for turning its broadside parallel to the flow direction. For E=0.32 ($\lambda_1 = 0.2$), we observed that the two disks form a stable vertical chain as shown in Fig. 6, which indicates that the critical value of the elasticity number for having a vertical chain is somewhere between 0.256 and 0.32.

To find more information about the two disk dynamics, we have varied the relaxation time $\lambda_1$ (resp., the elasticity number) from 0.01 to 1 (resp., from 0.016 to 1.6). For E between 0.016 ($\lambda_1$=0.01) and 0.24 ($\lambda_1$=0.15), the two disks stay separated and their interaction is periodical. In the phase space, based on the distances between each disk mass center and
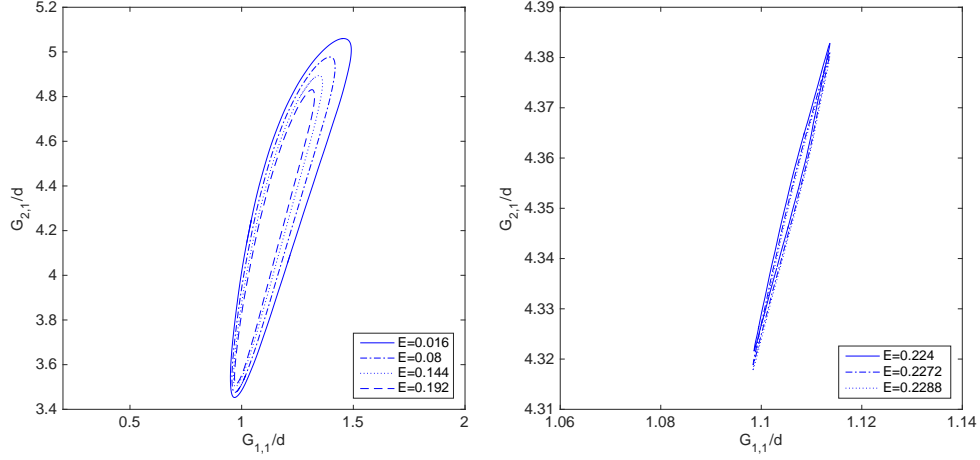
Figure 7: The limit cycles for $\rho_s = 1.0025$ in phase space: The periods of the two disks interacting apart are 58.55, 56.80, 55.485, 54.205, 52.067, 49 and 47.9 for E=0.016, 0.080, 0.144, 0.192, 0.224, 0.2272 and 0.2288, respectively.
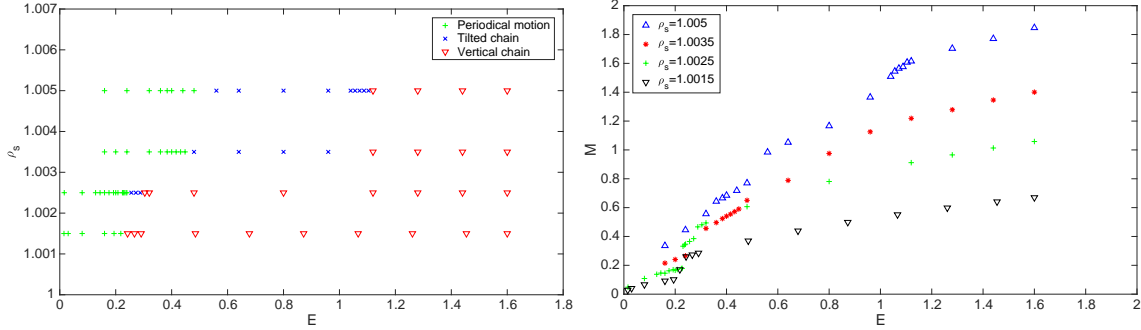


Figure 8: Phase diagram (top) and associated values of the Mach number (bottom) for two disk interacting in a narrow vertical channel for $\rho_s = 1.0015$, 1.0025, 1.0035 and 1.005.

the left sidewall, the attractor is a limit cycle for each value of the elasticity number shown in Fig. 7. At E=0.208 ($\lambda_1$=0.13), the limit cycle shrinks to about a point. Actually another kind of limit cycle occurs for $0.208 < E \leq 0.2288$ (see Fig. 7). But for $0.2304 \leq E \leq 0.24$, the two disks settle without noticeable periodic motion and remain separated at a constant distance. The gap between the two disk decreases when increasing the value of E from 0.2304 to 0.24. For E=0.256 ($\lambda_1 = 0.16$) and 0.288 ($\lambda_1$ =0.18), the two disks form a chain with a stable tilt angle of 29.69 and 82.33 degrees, respectively (see Fig. 5 for E=0.256). Finally, for E between 0.304 ($\lambda_1$=0.19 ) and 1.6 ($\lambda_1$=1), the two disks form a vertical chain. Thus the critical value of the elasticity number for having the formation of a vertical chain is somewhere in the interval [0.288, 0.304].

For the particles of density $\rho_s$=1.0015, similar particle motions are obtained. For E $\leq 0.2182$, the two disks stay separated and interact periodically. This periodic motion is

just like the one in Fig. 4 and its associated limit cycle is similar to those in the left plot in Fig. 7. For E between 0.2424 and 1.0667, the orientation of the disk chain oscillates first and then turns into the vertical direction after the oscillations damp out (e.g., see the trajectories of two disks for E=0.2424 and 0.4848 shown in Fig. 9). For E between 1.2606 and 1.6, the two disks form a chain which turns its orientation into the falling direction right away. No tilted chain is obtained for the values of the elasticity number considered in the phase diagram presented in Fig. 8. The critical value of the elasticity number for having a vertical chain formation is somewhere in the interval [0.2182, 0.2424].
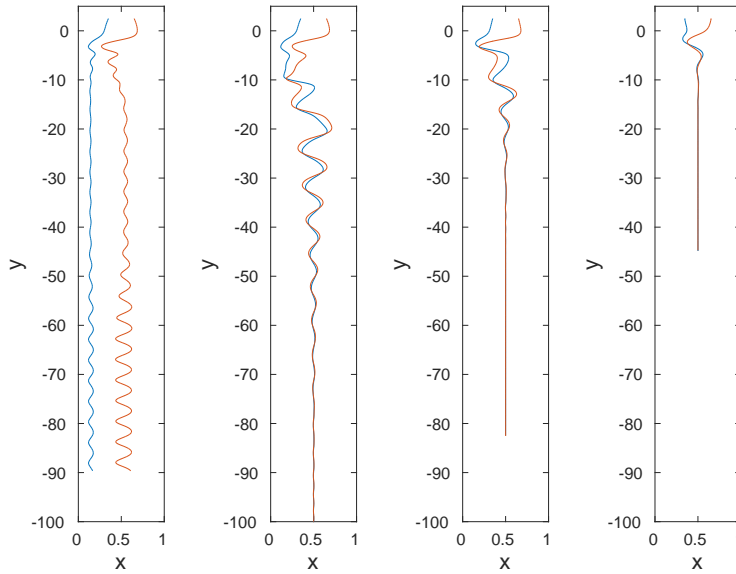


Figure 9: Trajectories of the two disk centers for $\rho_s = 1.0015$ at E=0.1393, 0.2424, 0.4848 and 0.12606 (from left to right).

For the particle densities $\rho_s$= 1.0035 and 1.005, we have also obtained similar kinds of particle motion for various values of the elasticity number as shown for both $\rho_s$=1.0015 and 1.0025 in Fig. 8. However the elasticity number range for having a tilted chain is wider. Also for these relatively heavier disks, besides the typical periodical motion discussed in the above cases, there is another one which we call "drafting, kissing and non-chaining" (see Fig. 10). The limit cycles of those two types of periodic motion for $\rho_s$=1.005 are shown in Fig. 11. The limit cycles in the left plot in Fig. 11 are associated with a motion like the one in Fig. 4 and those in the right plot are associated with the drafting, kissing and non-chaining. The particle positions and trajectories for $\rho_s$=1.005 and E=0.4 shown in Fig. 10 tell us that every time a chain is about to be formed after drafting and kissing between two disks, the two disk "long body" turns and then the two disks break away. We believe that the inability of the two disks to form a chain is due to the weakness of the elastic forces; indeed, for E = 0.56, a quasi horizontal and stable chain is formed (see Fig. 12). By comparing the particle positions shown in Figs. 10 and 12, we observe that the two particles touch ("kiss") each other between $t = 40$ and 48 for E=0.4 and 0.56. Then the pair in Fig. 10 breaks up at $t = 52$ for E=0.4, but the pair remains chained for E=0.56.
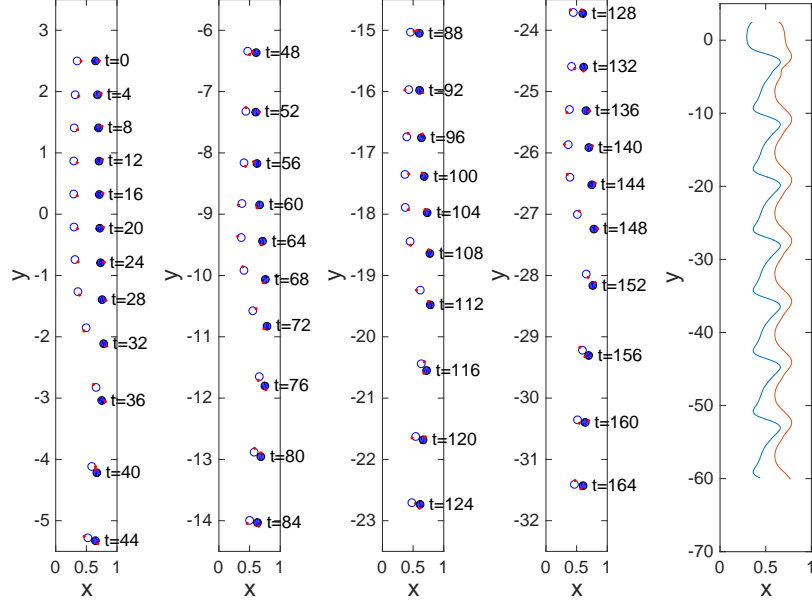
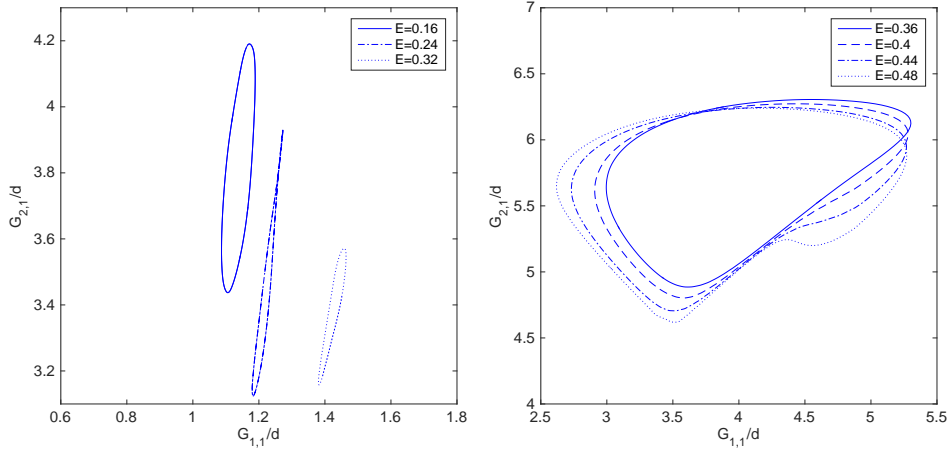Figure 10: Positions of the two disks drafting, kissing, and non-chaining for $\rho_s = 1.005$ and E=0.4.



Figure 11: The limit cycles for $\rho_s = 1.005$ in phase space: The periods of the two disks interacting apart are 21.65, 18.05 and 16.28 for E=0.16, 0.24 and 0.32, respectively (left) and the periods of two disks drafting, kissing, and not-chaining are 34.2, 38.45, 46.45 and 64 for E=0.36, 0.4, 0.44 and 0.48, respectively (right).
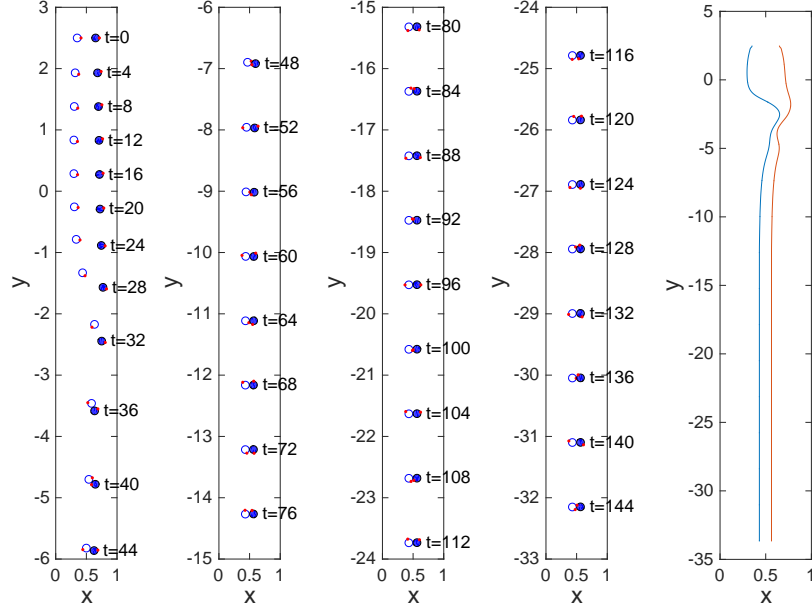
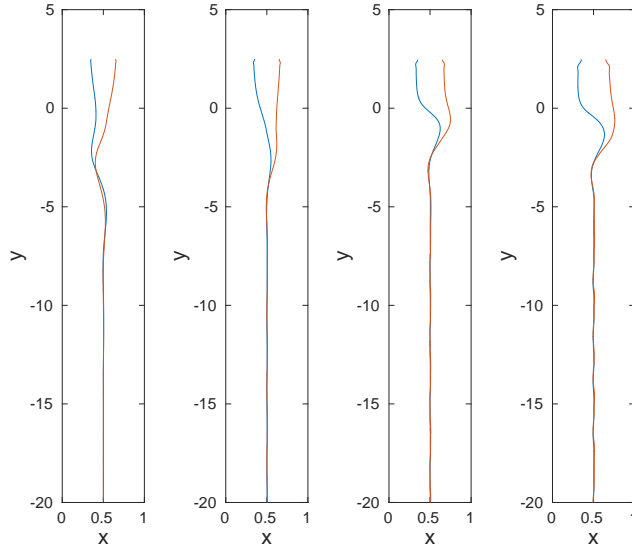Figure 12: Positions of two disks forming an almost horizontal chain for $\rho_s = 1.005$ at E=0.56.



Figure 13: Trajectories of the two disk centers forming vertical chains for E=1.6 and the density $\rho_s = 1.0015, 1.0025, 1.0035$ and $1.0045$ (from left to right).
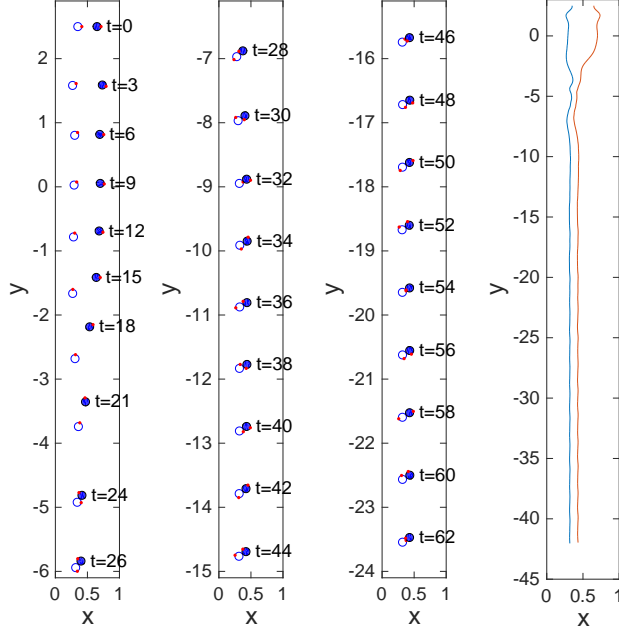
Figure 14: Positions of the two disks forming a tilted chain (left three) and trajectories (right) of the two disks for $\rho_s = 1.01$ and E=1.6 and M=3.0784.

All the values of the Mach number associated with the different values of the particle density $\rho_s$ and elasticity number are presented in Fig. 8. For each fixed value of the elasticity number E, when the particle is heavier, the Mach number is increased. For example, at E=1.6, the two disks form a chain whose orientation turns vertical right away for the four particle densities considered here (see Fig. 13). The associated values of the Mach number for these four cases are 0.6697, 1.0582, 1.4004 and 1.8468 for $\rho_s$ =1.0015, 1.0025, 1.0035 and 1.005, respectively. As discussed in [6], the long body flips falling broadside-on for Mach number greater than its critical value ($O(1)$). To see the effect of the larger value of the Mach number on the chain orientation, we have increased the particle density to $\rho_s$=1.01 so that the particle settling velocity becomes faster. For E=0.16, 0.32 and 0.48, two heavier disks stay apart and interact periodically. But they form a tilted chain for E=0.64, 0.80 and 0.96. At E=1.12, a vertical chain is obtained and its associated Mach number is M=2.7343. For E=1.28, 1.44 and 1.6, chains with the tilted angles 32.23, 31.59 and 32.63 degrees are obtained and the associated values of the Mach number are 2.6879, 2.8660 and 3.0784, respectively. The Mach number at E=1.28 is less than the one at E=1.2 since the titled chain of two disks at E=1.28 has a slightly slower terminating settling speed than that of the vertical chain at E=1.2. The particle position and trajectories for E=1.6 are shown in Fig. 14. Thus a tilted chain can be obtained for the higher values of the Mach number while for the cases of those lower particle densities at the same elasticity number, vertical chains are obtained at E=1.28, 1.44 and 1.6 in Fig. 8. This result is consistent with those cases where an elliptic particle is settling in an Oldroyd-B fluid, as shown in [6], even though the chain of two disks is not a rigidly connected dipole. The values of the elasticity and Mach numbers determine whether a two disk chain can be formed and the chain orientation.
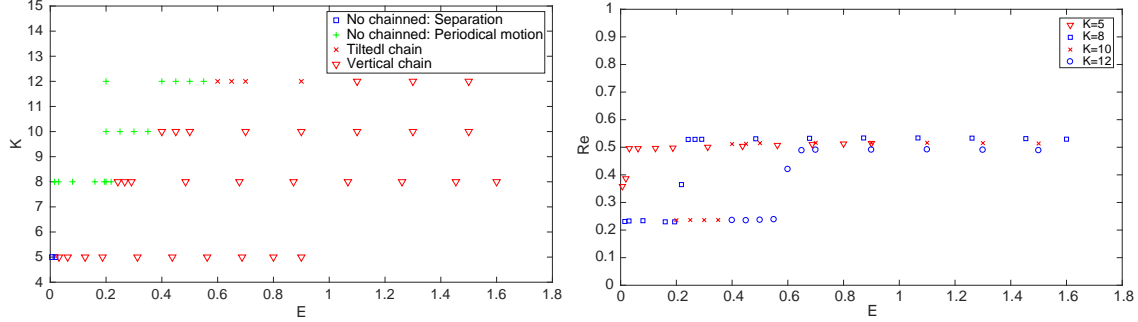
13

Figure 15: Phase diagram (left) and associated values of the Reynolds number (right) for two disks interacting in a vertical channel with different confined ratios.

Concerning the wall effect on the formation of two disk chains, we have investigated the cases of different values of the blockage ratio defined by $K = H/d$ where $d$ is the diameter of the two same size disks and $H$ is the width of the channel. For all aforementioned results, the blockage ratio is $K = 1/0.125 = 8$. The particle density considered here is $\rho_s = 1.0015$. All other parameters are the same with the exception of the disk diameter, fluid viscosity and mesh size. The diameters are $1/12$, $1/10$, $1/8$, and $1/5$; the associated fluid viscosities being $1/25$, $1/40$, $1/50$ and $1/60$ and the mesh size for the velocity field being $1/128$, $1/128$, $1/196$ and $1/196$, respectively. In order to reduce the effect of the particle Reynolds number (i.e., of the terminal particle speed) on the formation of vertical chains, we have adjusted the fluid viscosity so that the particle Reynolds numbers are about the same for those cases having vertical chains formed (see Fig. 15). We have obtained the same types of disk interaction when two disks sediment in the vertical channel for various values of the relaxation time as shown in Fig. 15. The wall effect does help two disks to form a vertical chain in a narrower channel at lower elasticity numbers; but the vertical chain is always formed for those cases at higher elasticity numbers presented in Fig. 15. When two disks have periodic interaction, the disk rotation synchronizes with its translation velocity. e.g., those of the case of K=10 at E=0.2 are shown in Fig. 16. When reducing the value of blockage ratio $K$, the period of the two disk interaction at the lower elastic number is also reduced, e.g., for the cases of E=0.2 shown in Fig. 15, the periods are 113.07, 100.2 and 91.29 for K=12, 10 and 8, respectively, and there is no periodic motion but a vertical chain for K=5. When reducing the value of $K$, the rotating speed of the disk close to the right wall is increasing slightly and the one in the middle of the channel does not change much as shown in Fig. 16, .

Since having identical disks is never the case experimentally, we have varied the diameter of one disk to find out its effect on the two disk interaction. The other one has a fixed diameter 0.125. All other parameters are the same as those of the particle density $\rho_s = 1.0035$. As shown in Fig. 17, having a disk of 10% larger in diameter does increase the range of having vertical chain and suppress the range of no chaining and periodic motion. For the other case of having a 10 % smaller diameter, we have obtained almost the same result. But for the cases of the 5% change in diameter, the effect is qualitatively the same but weaker. The mass center of the relative larger disk is always lower than that of the
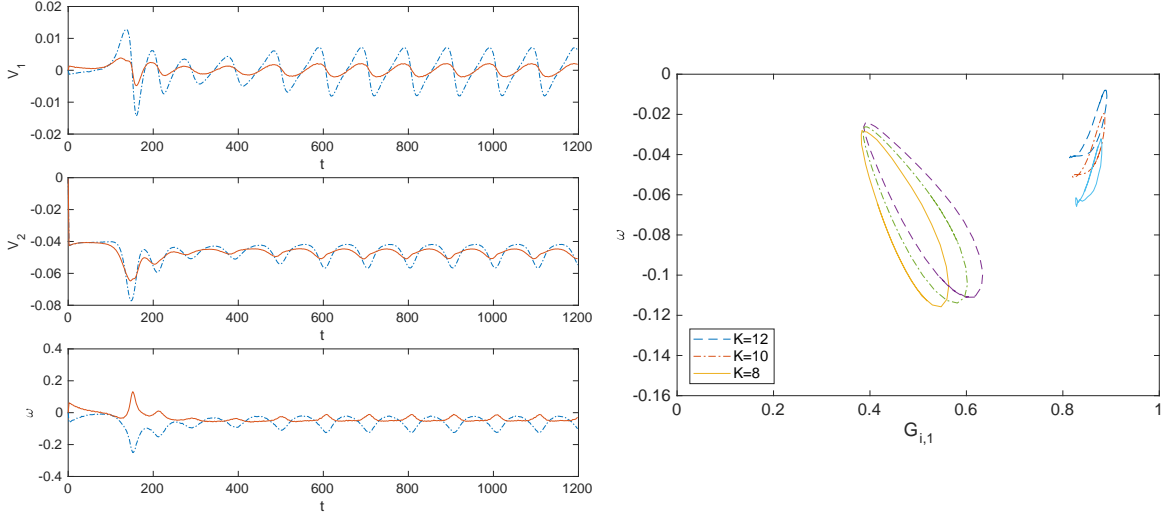
14

Figure 16: Left: Histories of the two disk horizontal velocity (left top), vertical velocity (left middle), angular velocity (left bottom) for $\rho_s = 1.0015$, $d = 0.1$, $K = 10$ and E=0.2. Right: The limit cycles for the angular velocity and the horizontal position of the disk mass center for $K = 8$ (solid line), 10 (dashed-dotted line) and 12 (dashed line).
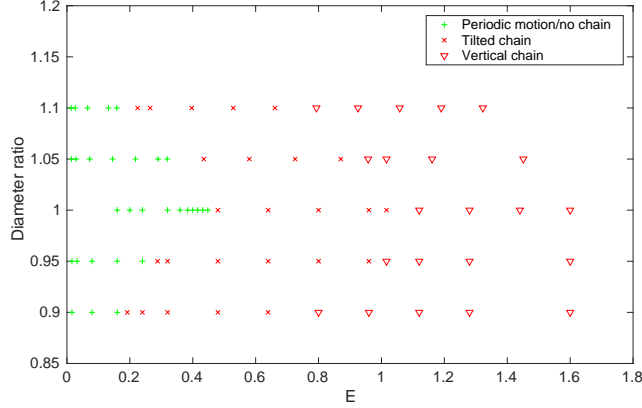


Figure 17: Phase diagram for two different size disks interacting in a vertical channel: One disk has a fixed diameter of $d = 0.125$ and the other one has $0.9d$, $0.95d$, $d$, $1.05d$ and $1.1d$ (from bottom to top in the plot) .

smaller one during the interaction for all cases.

To compare the difference between the dynamics of two rigidly connected disks and that of two freely moving disks, we have considered the cases associated with the particle density $\rho_s = 1.0025$ discussed at the beginning of the this Section (see Figs. 3–8). All the parameters are the same except that the two disks are rigidly connected while settling in the channel. The numerical results show that for E between 0.08 and 1.6, the orientation of the long body of two rigidly connected disks is parallel to the direction of sedimentation. The critical value of the elasticity number for having such orientation is much less than the

15

one, E=0.304, for the case of two freely moving disks. This result is not surprising since the chain of two freely moving disks is not really a long rigid body. For E between 0.04 and 0.07, a tilted orientation is obtained for the two rigidly connected disks. For E ≤ 0.03, the two disk long body oscillates between two different orientations (e.g., see Fig. 18 for E=0.02). This oscillation is not seen among the dynamics of two freely moving disks shown in Figs. 3–8 also due to the fact that the chain of two freely moving disks is not really a long rigid body.
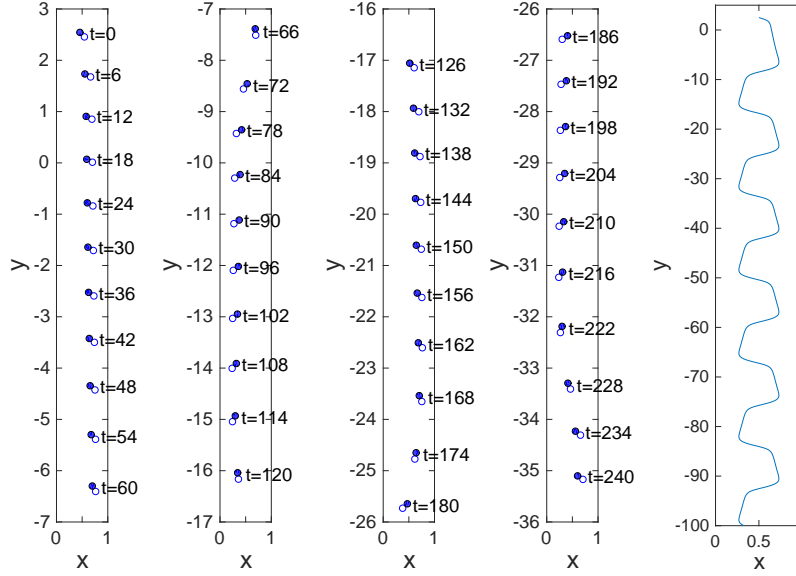


Figure 18: Positions and orientations of the two rigidly connected disks (left four) and trajectory of the long body mass center (right) for $\rho_s = 1.0025$ and E=0.02.

*Remark* 3.1. In all simulations presented in this article, the two disks are initially located at the same height. We believe that the results might be slightly different if using different initial configurations and different blockage ratios. For example, in [12], two balls were released at the same height with different distance between them in a quasi-two dimensional channel to study the critical distance for having the formation of two ball chain. The effect of the horizontal distance between two disks on the formation of two disk chain and the effect of other initial positions are worth a further study. Concerning the interactions of more than two settling disks in Oldroyd-B fluids, a recent study of multiple disk chains in [29] indicates that the formation of three or more disk chains in Oldroyd-B fluids relies on the elasticity number value. A next step would be to study the formation of long particle chains in Oldroyd-B fluids versus the elasticity number.

Even in two dimensions, all numerical results in this article look like some of the interactions of two balls in three dimensions and can help understanding how particle interact in a three-dimensional channel. For example, it is known that the behavior of particles settling in a Newtonian viscous fluid may be quite different from the one of particles settling in a viscoelastic fluid. Indeed, a well-known behavior for two balls settling in a Newtonian viscous fluid is the so-called drafting, kissing and tumbling phenomenon [22], while two

16

balls settling in an Oldroyd-B fluid exhibit the kissing, drafting and chaining phenomenon [12]. The kissing, drafting and chaining of two disks obtained in this article looks like that of two balls settling in a quasi-two-dimensional channel reported in [12]. The generalization of the computational methodology used in this article to three-dimensions is in progress, the investigation of the interaction of two and more balls settling in a vertical channel filled with an Oldroyd-B fluid will be submitted for publication in a near future.

# 4    Conclusion

In this article we have presented a numerical study of the dynamics of two disks settling in a narrow vertical channel filled with an Oldroyd-B fluid. For the cases considered in this article, two kinds of particle dynamics were observed, namely: (i) a periodic interaction between the two disks and (ii) the formation of a two disk chain. For the periodic interaction, two different motions are observed: (a) the two disks stay far apart and their interaction is periodical (as shown in Fig. 4), which is similar to one of the motions reported in [23], and (b) the two disks draft, kiss and break away periodically, chains not being formed, due to the weakness of the elastic forces. When, for larger values of E, a chain is forming, it is either a tilted chain or a vertical one. A tilted chain can be obtained if either the elasticity number value is less than the critical one associated with vertical chain formation, or if the Mach number is greater than a critical value. Hence the values of the elasticity number and the Mach number determine whether the chain of two disks can be formed and its orientation. Numerical results also show that the wall effect enhances the formation of the vertical chain of two disks in a narrower channel.    For two disks of slightly different sizes, it is easier for them to form a chain when comparing with the case of two identical disks. When comparing with the dynamics of two rigidly connected disks sedimenting in an Oldroyd-B fluid, the critical elasticity number for having vertical chains of two disks is much higher than that for two rigidly connected disks since the chain of two disks is not really a long rigid body.

# References

[1] R. P. Chhabra, *Bubbles, Drops, and Particles in Non-Newtonian Fluids* (CRC Press, Boca Raton, FA, USA, 1993).

[2] G. H. McKinley, "Steady and transient motion of spherical particles in viscoelastic liquids," in *Transport Processes in Bubbles, Drops and Particles*, edited by R.P. Chhabra, D. De Kee (Taylor & Francis, New York, NY, 2002), 2nd ed., p. 338.

[3] M. J. Economides and K. G. Nolte, *Reservoir Stimulation* (Prentice Hall, Englewood Cliffs, NJ, USA, 1989).

[4] J. Feng, P.Y. Huang, and D.D. Joseph, "Dynamic simulation of sedimentation of solid particles in an Oldroyd-B fluid," J. Non-Newtonian Fluid Mech. **63**, 63 (1996).

[5] H.H. Hu, N.A. Patankar, and M.Y. Zhu, "Direct numerical simulations of fluid-solid systems using the arbitrary Lagrangian-Eulerian technique," J. Comput. Phys. **169**, 427 (2001).

[6] P. Y. Huang, H. H. Hu, and D. D. Joseph, "Direct simulation of the sedimentation of elliptic particles in Oldroyd-B fluids," J. Fluid Mech. **362**, 297 (1998).

[7] P. Singh, D. D. Joseph, T. I. Helsa, R. Glowinski, and T.-W. Pan, "A distributed Lagrange multiplier/fictitious domain method for viscoelastic particulate flows," J. Non-Newtonian Fluid Mech. **91**, 165 (2000).

[8] Z. Yu, N. Phan-Thien, Y. Fan, and R. I. Tanner, "Viscoelastic mobility problem of a system of particles," J. Non-Newtonian Fluid Mech. **104**, 87 (2002).

[9] X.M. Shao and Z.S. Yu, "Sedimentation of circular particles in Oldroyd-B fluid," J. Hydrodynamics **16**, 254 (2004).

[10] J. Hao, T.-W. Pan, R. Glowinski, and D. D. Joseph, "A fictitious domain/distributed Lagrange multiplier method for the particulate flow of Oldroyd-B fluids: A positive definiteness preserving approach," J. Non-Newtonian Fluid Mech. **156**, 95 (2009).

[11] G. D'Avino and P.L. Maffettone, "Particle dynamics in viscoelastic liquids," J. Non-Newtonian Fluid Mech. **215**, 80 (2015).

[12] D.D. Joseph, Y.J. Liu, M. Poletto, and J. Feng, "Aggregation and dispersion of spheres falling in viscoelastic liquids," J. Non-Newtonian Fluid Mech. **54**, 45 (1994).

[13] R. Glowinski, T.-W. Pan, T. I. Hesla, D. D. Joseph, and J. Périaux, "A fictitious domain approach to the direct numerical simulation of incompressible viscous fluid flow past moving rigid bodies: application to particulate flow," J. Comput. Phys. **169**, 363 (2001).

[14] R. Glowinski, "Finite element methods for incompressible viscous flows," in *Handbook of Numerical Analysis*, edited by P.G. Ciarlet, J.L. Lions (North-Holland, Amsterdam, 2003), vol. IX, p. 3.

[15] S. Hou, T.-W. Pan, and R. Glowinski, "Circular band formation for incompressible viscous fluid-rigid-particle mixtures in a rotating cylinder," Phys. Rev. E **89**, 023013 (2014).

[16] F. P. T. Baaijens, "Mixed finite element methods for viscoelastic flow analysis: A review," J. Non-Newtonian Fluid Mech. **79**, 361 (1998).

[17] R. Keunings, "A survey of computational rheology," in *Proc. 13th Int. Congr. on Rheology*, edited by D. M. Binding et al. (British Society of Rheology, Glasgow, United Kingdom, 2000), Vol. 1, p. 7.

[18] R. Fattal and R. Kupferman, "Constitutive laws for the matrix-logarithm of the conformation tensor," J. Non-Newtonian Fluid Mech. **123**, 281 (2004).

[19] R. Fattal and R. Kupferman, "Time-dependent simulation of viscoelastic flows at high Weissenberg number using the log-conformation representation," J. Non-Newtonian Fluid Mech. **126**, 23 (2005).

[20] Y.-L. Lee and J. Xu, "New formulations, positivity preserving discretizations and stability analysis for non-Newtonian flow models," Comput. Methods Appl. Mech. Eng. **195**, 1180 (2006).

[21] A. Lozinski and R.G. Owens, "An energy estima te for the Oldroyd-B model: theory and applications," J. Non-Newtonian Fluid Mech. **112**, 161 (2003).

[22] A. F. Fortes, D. D. Joseph, and T. S. Lundgren, "Nonlinear mechanics of fluidization of beds of spherical particles," J. Fluid Mech. **177**, 467 (1987).

[23] C. K. Aidun and E. J. Ding, "Dynamics of particle sedimentation in a vertical channel: Period-doubling bifurcation and chaotic state," Phys. Fluids **15**, 1612 (2003).

[24] D. D. Joseph, *Fluid Dynamics of Viscoelastic Liquids* (Springer, New York, NY, USA, 1990).

[25] E. J. Dean and R. Glowinski, "A wave equation approach to the numerical solution of the Navier-Stokes equations for incompressible viscous flow," C.R. Acad. Sci. Paris, Série I, **t. 325**, 783 (1997).

[26] Y. L. Liu and D. D. Joseph, "Sedimentation of particles in polymer solutions," J. Fluid Mech. **255**, 565 (1993).

[27] H.H. Hu, D. D. Joseph, and M. J. Crochet, "Direct simulation of fluid particle motions," Theoret. Comput. Fluid Dynamics **3**, 285 (1992).

[28] T.-W. Pan, R. Glowinski, and G. P. Galdi, "Direct simulation of the motion of a settling ellipsoid in Newtonian fluid," J. Comput. Applied Math. **149**, 71 (2002).

[29] T.-W. Pan R. Glowinski, "Dynamics of particle sedimentation in viscoelastic fluids: A numerical study on particle chain in two-dimensional narrow channel," J. Non-Newtonian Fluid Mech. **244**, 44 (2017).